Spurious correlations in simultaneous EEG-fMRI driven by in-scanner movement

M.-C. Fellner[1,2], G. Volberg[3], K. J. Mullinger[4, 5], M. Goldhacker[3], M. Wimber[4], M. W. Greenlee[3], S. Hanslmayr[1, 4]

[1] Universität Konstanz, Fachbereich Psychologie, Postfach 905, 78457 Konstanz, Germany

[2] Ruhr University Bochum, Department of Neuropsychology, Institute of Cognitive Neuroscience, 44801 Bochum, Germany

[3] Universität Regensburg, Psychologie, 93040 Regensburg, Germany

[4] University of Birmingham, Edgbaston, Birmingham B15 2TT, United Kingdom

[5] University of Nottingham, Sir Peter Mansfield Magnetic Resonance Centre, Nottingham NG7 2RD, United Kingdom

Corresponding Author: Marie-Christin Fellner, marie-christin.fellner@rub.de

Present address: Ruhr University Bochum
Department of Neuropsychology
Institute of Cognitive Neuroscience,
44801 Bochum, Germany

Abstract

Simultaneous EEG-fMRI provides an increasingly attractive research tool to investigate cognitive processes with high temporal and spatial resolution. However, artifacts in EEG data introduced by the MR-scanner still remain a major obstacle. This study employing commonly used artifact correction steps shows that head motion, one overlooked major source of artifacts in EEG-fMRI data, can cause plausible EEG effects and EEG-BOLD correlations. Specifically, low frequency EEG (<20 Hz) is strongly correlated with in-scanner movement. Accordingly, minor head motion (<0.2 mm) induces spurious effects in a twofold manner: Small differences in task-correlated motion elicit spurious low frequency effects, and, as motion concurrently influences fMRI data, EEG-BOLD correlations closely match motion-fMRI correlations. We demonstrate these effects in a memory encoding experiment showing that obtained theta power (~3-7 Hz) effects and channel-level theta-BOLD correlations reflect motion in the scanner. These findings highlight an important caveat that needs to be addressed by future EEG-fMRI studies.

Keywords: brain oscillations, EEG-BOLD correlations, motion artifacts, simultaneous EEG-fMRI, theta oscillations

Highlights

- Motion causes spurious effects using common artifact correction in EEG- fMRI analysis
- Spurious motion effects resemble neurophysiological plausible effects
- Minor task related motion can cause spurious task related EEG effects
- Motion-BOLD and EEG- BOLD correlations are largely overlapping after convolution with the HRF

1 Introduction

Simultaneous EEG and fMRI recordings provide an immensely useful neuroimaging technique as they offer the unique possibility to non-invasively record neural activity at highest temporal and spatial resolution (Debener et al., 2006). Such rich multidimensional datasets allow for numerous ways of merging EEG and fMRI data (Huster et al., 2012) with the most popular approach being EEG-informed fMRI analysis. Here, EEG parameters of interest are used to create a model of the BOLD responses. BOLD signals can be correlated with ERP components (Debener et al., 2005), resting state alpha power (Goldman et al., 2002) or task-related oscillatory power changes (Hanslmayr et al., 2011). Resulting spatial maps provide regions in which BOLD signal changes correlate with EEG parameters indicating a common generator of BOLD and EEG signals.

However the biggest restraining factor in simultaneous recordings is still the quality of the EEG data. Usually two types of artifacts are considered: the gradient and ballisto-cardio-graphic (BCG) artifacts (Allen et al., 1998; Debener et al., 2008; Liu et al., 2012a; Mullinger et al., 2013; Niazy et al., 2005). Another major source of artifact, spontaneous movement, is rarely discussed. Motion is a general problem for simultaneous recordings, since movement of any conductive material (i.e. EEG electrodes and wires) in a static magnetic field (as in an MR scanner) causes electromagnetic induction and consequently an artifactual EEG signal. Therefore, even very minor head motion on a sub-millimeter level severely affects the EEG, as for example the tiny movements related to every heartbeat are visible in the EEG data as BCG (Debener et al., 2008; Mullinger et al., 2013). Most researchers employing EEG-fMRI accept that these artifacts remain to some extent in their data, even after careful preprocessing, implicitly assuming that those artifacts are mainly decreasing the signal to noise ratio but not introducing spurious effects. This logic fails when head motion is correlated with the task parameters of interest (i.e. paradigm, behavioral performance, BOLD signals). Since it is well known that fMRI-BOLD signals are correlating with motion (voluntarily or physiologically driven), BOLD-motion correlations might be a serious concern for EEG-fMRI correlations (Birn et al., 1999; Friston et al., 1996; Murphy et al., 2013; Power et al., 2014).

We here present data measuring EEG data inside and outside an MR-scanner. EEG and simultaneous EEG-fMRI data were recorded during a memory paradigm where we focused on theta

oscillations and their relation to BOLD signals (Figure 1A). The memory relevant aspects of this dataset will be reported in detail elsewhere (Fellner et al., in prep) and are only in so far relevant for this study as motion induced spurious "memory-like" effects. Specifically, we demonstrate that: (i) In-scanner EEG data on electrode level is highly dominated by motion related artifacts. (ii) Task related motion in-scanner can cause spurious task related EEG power effects that are in stark contrast to artifact-free out-of-scanner data. (iii) In-scanner motion can drive spurious, but neurophysiologically plausible EEG-BOLD correlations.

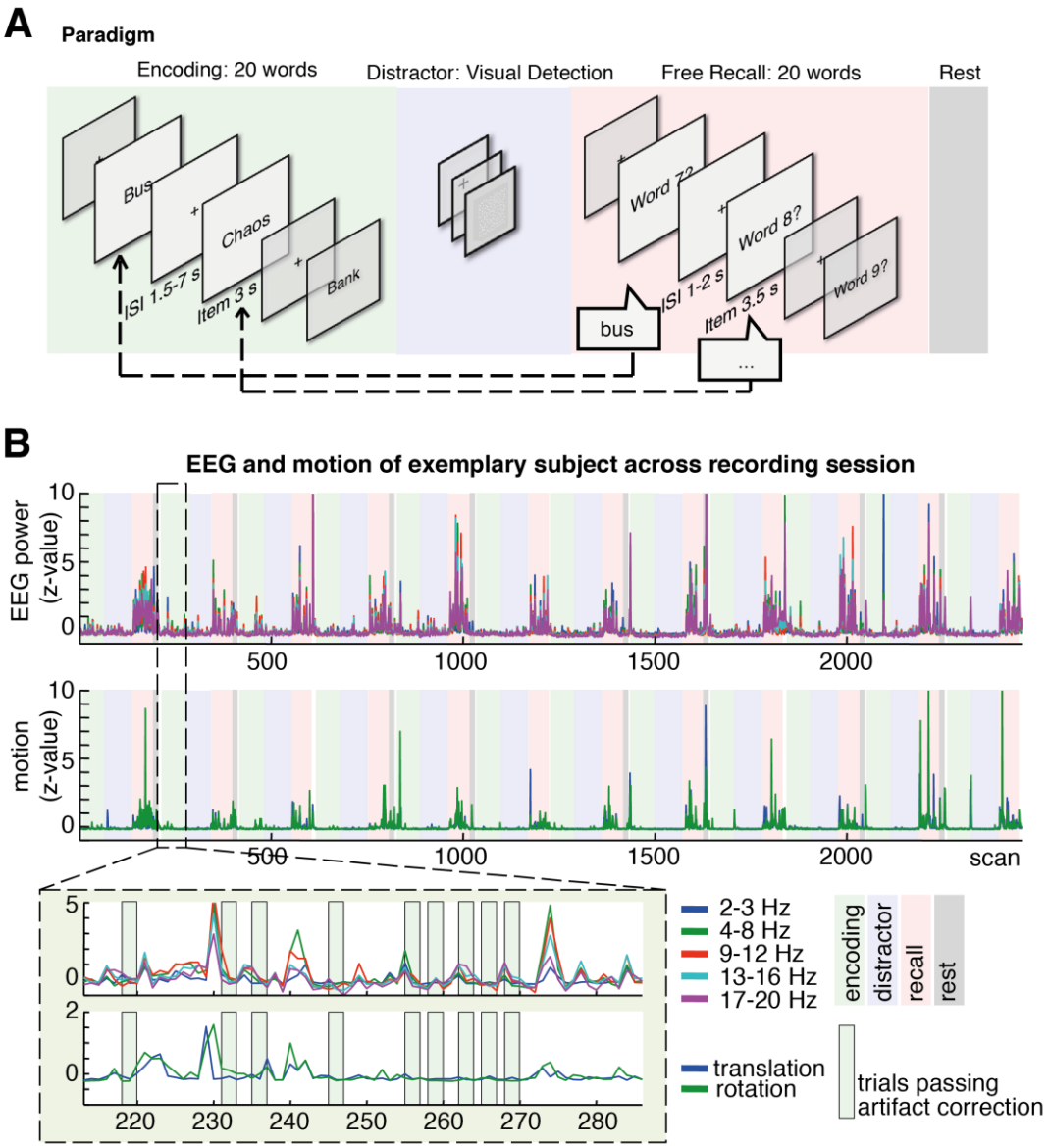

Figure 1: Paradigm and exemplary oscillatory power and motion timecourses

(A) The experiment consisted of 12 study-recall cycles, each of these cycles consisted of an encoding phase, a visual detection task, which served as a memory distractor, a free recall phase and a short rest period, in which participants were allowed to relax, move and close their eyes. During recall participants verbally recalled items presented in the previous encoding phase. Items during encoding were classified as later remembered or forgotten according to those responses. (B) Power time courses of different frequency bands and motion parameters mp_z during the whole scanning session of one exemplary participant. EEG closely resembles motion throughout all four task phases. Task phases are indicated by the shaded background colors matching coloring in (A). Epochs of interest in this experiment were encoding phases highlighted by green boxes. An exemplary encoding epoch is highlighted by dashed lines and shown in close-up. Encoding phases exhibited no exceedingly high motion and only low motion encoding trials that passed artifact correction highlighted by green boxes passed visual artifact inspection and were subjected to further encoding analyses.

2 Methods

2.1 Participants

The same memory encoding paradigm was measured in two different setups: in one group of twenty-five participants simultaneous EEG-fMRI was recorded (in-scanner data), whereas another group of thirty volunteers participated in an EEG-only study (out-of-scanner data). In-scanner data from three participants had to be excluded because of poor data quality, one participant had to be excluded because of a missing structural scan and data from another two participants did not provide enough items in one of the memory conditions, resulting in a sample of nineteen in-scanner datasets (mean age=22.95, 12 female). In out-of-scanner data eight participants had to be excluded because of low trial numbers resulting in twenty-two out-of-scanner datasets (mean age=20.2 yrs, 12 female). All participants spoke German as their native language, reported no history of neurologic or psychiatric disease, and had normal or corrected to normal vision.

2.2 Paradigm

Participants in both datasets participated in the identical experiment. The experiment consisted of twelve repeated memory encoding-recall cycles including an encoding phase, a distractor phase, a free recall memory test and a short rest period (see Figure 1). In each encoding phase the participants' task was to memorize 20 words. Each encoding-recall cycle ended with a 20 sec rest period in which participants were allowed to relax (blink, etc.). During encoding participants were instructed to use two differing mnemonic strategies: The method of loci and the pegword method. Both encoding conditions are cognitively demanding and call for high levels of attention. Both conditions showed no difference in spurious oscillatory activity and movement pattern and therefore data was merged for the current analysis. Each to-be-encoded word was presented for 3 sec followed by fixation cross presented with an exponential jitter from 1.5-7 sec to improve design efficiency for event-related fMRI analysis. The encoding phase was followed by a visual detection task serving as a distractor task (similar task as reported in Hanslmayr et al., 2013). In the following free recall phase participants were asked to recall all 20 words as presented during the preceding encoding phase. Recall performance

was used to classify encoding trials as subsequently remembered or forgotten. In scanner, verbal responses were recorded using an MRI-compatible microphone (MRconfon). Scanner noise was removed from the resulting audio files using the free software package Audacity (http://audacity.sourceforge.net/). In out-of-scanner EEG recordings recall performance was scored manually by the experimenter. Each experiment was split into 4 consecutive recording sessions to keep file sizes manageable.

Different word material was used for each study-test cycle counterbalanced across participants and between conditions. Participants remembered on average 48.7% (std= 0.12) of the words in the in-scanner dataset and 55.5% (std=0.13) in the out-of-scanner datasets, revealing a non significant tendency of higher recall rates out-of-scanner ($T(39)=1.757$, $p=0.087$).

2.3 EEG data-recording

The in-scanner EEG data were recorded from 63 channels in an equidistant montage, (EasyCap, Herrsching, Germany). An MR compatible amplifier (BrainAmp MR, Brain Products, Gilching Germany) together with the Syncbox device (Brain Products) was used to synchronize EEG recordings to the MR scanner clock. Recordings were referenced to Fz and later rereferenced to average reference (which excluded any noisy channels). Impedances were kept below 20 kΩ. ECG was recorded by an electrode placed below the left scapula. The signals were amplified between 0.1–250 Hz and a software filter with a low cutoff of 0.3Hz and high cutoff of 70Hz applied during acquisition. The EEG data were sampled at 5 kHz with a resolution of 0.5µV. Cables connecting cap and amplifiers were fixated by adhesive tape to prevent any additional movement-related artifacts. The same EEG amplifier and caps were used in both experiments (in-scanner and out-of-scanner). The only differences in recording between the two datasets concerned specific settings for simultaneous recordings: in the out-of-scanner data no syncbox was used, data was sampled at 500 Hz with a resolution of 0.5µV, no software filters were set and no ECG was recorded. During out-of-scanner recordings participants were sitting upright in front of a computer screen instead of in supine position in-scanner, where stimuli were presented on a mirror. Changes in body position have been shown to

affect resting state EEG in higher frequencies (>30 Hz), but not task related changes in lower frequency bands (Rice et al., 2013; Thibault et al., 2014).

2.4 fMRI data recording

After EEG preparation participants were placed in the scanner. Extra padding was placed surrounding the head of the participants to suppress head movements and discomfort caused by the EEG cap. Imaging was performed using a 3-Tesla MR head-only scanner (Siemens Allegra). During fMRI scanning, 2475-2480 whole-brain image volumes, consisting of 34 axial slices each, were continuously acquired using a standard T2*-weighted echo-planar imaging (EPI) sequence (repetition time TR=2000 ms; echo time TE=30 ms; flip angle=90°; 64x64 matrices; in-plane resolution: 3x3 mm; slice thickness: 3 mm, interleaved slice acquisition). High-resolution sagittal T1-weighted images were acquired after the functional scans, using a magnetization-prepared rapid gradient echo sequence (TR=2250 ms; TE=2.6 ms; 1 mm isotropic voxel size) to obtain a 3D structural scan. To prevent EEG artifacts caused by the helium pump and internal cooling of the scanner, both were switched off during the recordings.

2.5 EEG data preprocessing

The first preprocessing step for in-scanner EEG data was to reduce scanner-induced gradient artifacts. The EEGLAB plug-in FMRIB (www.sccn.ucsd.edu/eeglab, (Niazy et al., 2005) was used to reduce gradient artifacts. Synchronisation of scanner clocks by the syncbox ensured accurate sampling of the gradient artifact. BCG artifact correction involved two steps: heartbeat detection and BCG correction. At first, each heartbeat was identified by detecting QRS complexes in the ECG recording. Heartbeat detection was carried out using the FMRIB implemented method or AMRI-eegfmri-toolbox (https://amri.ninds.nih.gov/cgi-bin/software, (Liu et al., 2012a). For all but one dataset, the AMRI method provided a higher QRS detection performance revealed by average QRS-triggered-ECG ERPs and visual single trial inspection. OBS method was used to reduce the BCG artifact (Niazy et al., 2005).

For analysis of memory encoding effects, encoding phase data from both datasets, in-scanner and out-of-scanner, were epoched into trials -2.5 to 3.5 sec around item onset to provide sufficiently long

epochs for wavelet analysis. The epoched data was visually inspected, and trials containing residual scanner artifacts and other idiographic artifacts (channel jumps, muscle artifacts, noisy channels) were excluded from further analysis. Noisy channels were excluded in 4 datasets recorded out-of-scanner and in 3 datasets in-scanner, maximally 3 electrodes were excluded in each of these datasets. Infomax independent component analysis as implemented in Fieldtrip (www.ru.nl/fcdonders/fieldtrip, (Oostenveld et al., 2011) was applied to correct for residual artifacts (e.g. remaining gradient and BCG artifacts, eyeblinks, eye movements, or tonic muscle activity). The maximum number of independent components was estimated, equaling the number of channels in a dataset (59 to 62 ICs). On average 11.8 ICs were rejected owing to these residual artifacts in the in-scanner dataset (range: 9-17 ICs), 3.8 ICs were rejected in the out-of-scanner data (range:1-8 ICs). Note that the majority of in-scanner ICs are significant positively correlated to motion (see figure S2). Percent variance accounted for by the rejected ICs is shown in Figure S1, showing that a greater amount of the total variance is rejected from data acquired inside the scanner than outside the scanner, as expected from the additional noise sources. Remaining ICs were back projected to channel level. Data was again visually inspected for remaining artifacts and then subjected to further analysis. In in-scanner data, on average 62.05 hit trials (range 28-113) and 65.21 miss trials (range 34-115) passed the artifact corrections. It was also tested whether specific motion related ICs can be identified in order to remove motion related activity. However motion correlated positively with the majority of ICs, which prevented such a denoising approach (see Figure S2). Out-of-scanner runs consisted of an average of 107.55 hit trials (range 56-170) and 82.55 miss trials (range 41-142). Finally, for datasets with rejected electrodes prior to ICA, those channels were interpolated using neighboring electrodes.

2.6 fMRI data preprocessing

Image preprocessing and statistical analysis was performed using SPM8 (Wellcome Department of Cognitive Neurology, London: UK, www.fil.ion.ucl.ac.uk/spm). After discarding the first images of each session, time series were corrected for differences in slice acquisition time, and spatially realigned to the first image of the session. The realignment parameters obtained in this preprocessing

step were used to quantify movement in the latter analyses. The mean functional image was coregistered with the structural image, and all images were then normalized to the MNI brain (Montreal Neurological Institute, www.mni.mcgill.ca) using the normalization parameters determined from segmentation of the structural image. As a last step, images were smoothed with a Gaussian kernel of 8 mm FWHM.

2.7 EEG data analysis

For time frequency analysis, data were subjected to a wavelet transform as implemented in Fieldtrip (www.ru.nl/fcdonders/fieldtrip,). Data were filtered to obtain oscillatory power between 2 Hz and 30 Hz using wavelets with a 5 cycle length. Resulting data was z-transformed to the mean power and standard deviation across all trials of each respective frequency band and channel.

To identify time-frequency clusters showing significant differences between conditions, a sliding window cluster permutation test was used (for details, see (Staudigl and Hanslmayr, 2013). This procedure was used to analyze memory encoding effects (Figures 4 A&B) and to analyze power differences between high and low motion encoding trials (Figure 4 C). For each 300 ms x 1 Hz time bin a cluster permutation test, as implemented in Fieldtrip, was calculated (Maris and Oostenveld, 2007), which returned a p-value for each bin. To check if significant time clusters revealed in this analysis show continuous scalp topography, another cluster permutation test was performed on the respective time-frequency bin of these clusters.

2.8 Movement measure

A movement measure was calculated using fMRI realignment parameters. In the realignment procedure absolute displacement in 6 directions (*x, y, z* translations and 3 rotations: pitch, yaw and roll, here denoted as rp_i , i=1,..,6) of every MR volume s relative to the first MR volume is estimated. Realignment parameters represent absolute shifts in position relative to the first volume acquired in a given session and can be used to calculate a relative motion measure between consecutive scans. We combined realignment parameters of all dimensions (j=1, k=6) to a single normalized motion measure mp_z:

$$mp(s) = \sum_{i=j}^{k} \left(\left(\frac{rp_i(s+1) - M_{rp_i}}{std_{rp_i}} \right) - \left(\frac{rp_i(s) - M_{rp_i}}{std_{rp_i}} \right) \right)^2 \quad \text{Eq. 1}$$

$$mp_z(s) = \frac{mp(s) - M_{mp}}{std_{mp}} \quad \text{Eq. 2}$$

M and std denote the respective mean and standard deviations of the realignment parameter or combined motion parameter indicated in indices. Note that mp_z is calculated with the mean and standard deviations of the respective interval of interest: for analyses of motion across all scans (GLM-allmotion, Figure 1B upper plot, correlations in Figure 2A, Figure 3C) mean and std were calculated based on all scans; for analysis focusing on motion during certain epochs, i.e. encoding trials or low motion epochs (GLM-small motion, Figure 1B lower plot, Figure 2B, Figure 4C) mean and std were calculated based on all scans in these epochs.

Both motion types, rotation and translation, exhibited highly similar time courses (Figure 1B, translation: j=1, k=3; rotation: j=4, k=6). Albeit theoretically head rotations should cause the biggest artifact by cutting the magnetic flux, natural human head motion rotation co-occurs with translations explaining the similarity between both measures. Therefore, movement collapsed across all 6 motion parameters was used for all subsequent correlative analyses. To more closely identify the motion patterns related to the spurious correlations, we additionally report mean relative differences of each realignment parameter referred to as relative translation or relative rotation m_i (Figure 5).

$$m_i(s) = | rp_i(s+1) - rp_i(s) | \quad \text{Eq. 3}$$

For statistical analysis m_i is normalized to the respective mean and std in order to ensure comparable scaling.

$$m_{iz} = \frac{m_i(s) - M_{m_i}}{std_{m_i}} \quad \text{Eq. 4}$$

2.9 Movement analysis of EEG data

To investigate the relationship of oscillatory power and in-scanner motion, irrespective of condition, the continuous artifact corrected EEG recording was epoched from -500 ms to 2500 ms relative to each volume trigger in order to provide a sufficiently long epoch for wavelet analysis. The

resulting 2-second trials are temporally matched to a certain fMRI volume (i.e. realignment parameter and motion parameter). The out-of-scanner data were epoched into arbitrary consecutive 2-second epochs to create a comparable dataset. Those epochs were subjected to time frequency wavelet analysis specified above. The *z*-transformed mean power for each 2-s scan interval was calculated for 5 frequency bands (delta: 2-3Hz, theta 4-8Hz, alpha: 9-12Hz, beta1: 13-16Hz, beta2: 17-20Hz).

For in-scanner data EEG power and in-scanner motion mp_z were correlated for each participant, electrode, and frequency band. Spearman's correlations were used and extreme power values, *z* larger than 2 were excluded to prevent outlier driven correlations. To test if group level correlations significantly exceeded zero, and to investigate the scalp topographies of those correlations, correlation coefficients were first Fisher z-transformed, and then subjected to a two-stage permutation approach. In a first step Wilcoxon sign-ranked tests were carried out for each electrode testing if correlation coefficients are different from zero. Then, to correct this result for multiple comparisons across electrodes a permutation test was employed. The test used 1000 permutation runs shuffling the sign of the correlation coefficient randomly for each subject and electrode. After each run, a Wilcoxon-signed-rank test was calculated returning the number of electrodes showing a significant effect in a randomly distributed dataset. After 1000 permutation runs this procedure yields test distribution of the probability of a given number of significant electrodes in a sample with random correlations. This distribution was used to calculate the corrected p-value henceforth referred to a p_{corr}.

2.10 fMRI: power and movement correlations

To investigate correlations of BOLD signals with motion and EEG power several random-effects GLMs were set up. In EEG-fMRI GLMs, theta power was added as a regressor either throughout the scanning session (GLM-alltheta) or only during encoding trials that passed stringent artifact correction criteria (GLM-cleantheta). Realignment parameters were added as regressors of no interest only to GLM-cleantheta. In all other models we strived to identify effects of motion in the data and therefore omitted realignment parameters from the GLMs. In each GLM event-related regressors modeling remembered and forgotten trials for each encoding condition, task block regressors modeling rest periods, free recall periods for each encoding condition and the distractor task, and session-specific

block and drift regressors were included. GLMs differed only in the specific theta or motion regressor added. The EEG power regressors were down-sampled to match the TR. Motion or power of epochs of interest was normalized (z-transformed) and epochs omitted from the respective regressor were replaced with zeroes. Motion or power regressors were convolved with the HRF and orthogonalized relative to the task regressors to avoid regressor correlations.

In GLM-alltheta, a theta power regressor was added based on theta power across the whole experiment including theta power during high motion recall phases and irrespective of motion or other artifacts (after the standard cleaning methods outlined above). In GLM-allmotion, a motion regressor was added based on the combined motion parameter mp_z across the whole recording period.

For GLM-cleantheta, a theta regressor was built by averaging z-transformed power of all electrodes showing the positive theta encoding effect (see electrodes highlighted in Figure 4A) during all artifact free encoding trials. GLM-smallmotion was designed to capture only correlations of small motion with BOLD signals. A motion regressor mp_z was added including only scans in which none of the relative translational movements exceeded 0.2 mm. The analysis was restricted to those small movements that match movements occurring during encoding trials (see Figure 5).

GLM-cleanalpha and GLM-cleanbeta were matching GLM-cleantheta, except that in these models average alpha and beta power, respectively, was averaged across all electrodes, convolved and added to the GLM. Non-convolved models were matching GLM-alltheta, GLM-cleantheta and GLM-allmotion and GLM-small motion except that in here non-convolved (no convolution with HRF) theta power or motion regressors were added to the GLM.

3 Results

3.1 Low frequency power and motion in scanner

EEG power in-scanner is largely dominated by head motion throughout all four phases of the experiment (i.e. encoding, distractor, recall, and rest; see paradigm in Figure 1A). Figure 1B shows how EEG power in all lower frequency bands closely resembles translational and rotational head

motion during the scanning session. This close relationship is especially evident during the free recall phase, which was not considered a period of interest, due to the high levels of movement generated by verbal recall. However, motion and power also co-varied during the low motion encoding phase (highlighted dashed box, Figure 1B). Not all encoding phase data were analyzed, but only relatively low motion trials that passed visual inspection during artifact correction (highlighted in light green in Figure 1B, also see Figure 5 for absolute motion values). Rotational and translational motion measures are closely related and consequently were combined into one motion parameter in all following analyses. In line with the above single-subject observations, analysis across all participants revealed that EEG power and motion (combined motion parameter mp_z) are positively correlated across the whole experiment in all lower frequency bands (<20 Hz), even after exclusion of outlier trials with z-values of power exceeding z>2 (all frequency bands p_{corr} <0.001) and also during the artifact free encoding phase trials, where correlations are smaller but still highly significant (all frequency bands p_{corr} <0.001, Figure 2 shows the correlation topographies).

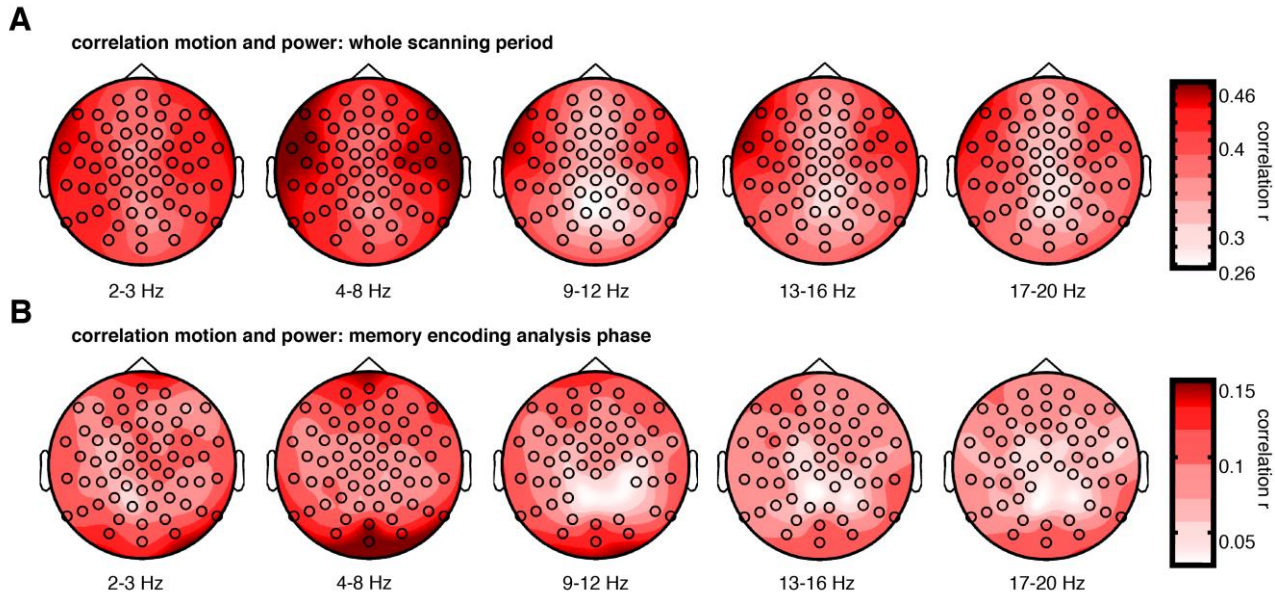

Figure 2: Scalp topographies of motion power correlations across frequencies

Power and motion are significantly positively correlated in all lower frequency bands. (A) Topography plots of Spearman correlation coefficients throughout the scanning sessions (outlier corrected for power z>2). (B) shows correlation of power and motion for used encoding trials only. Note that topographies of correlations do not vary across frequency bands. Correlations were more pronounced on the outermost electrodes resembling a ring like pattern; circles highlight electrodes showing significant differences. All p_{corr}´s<0.001

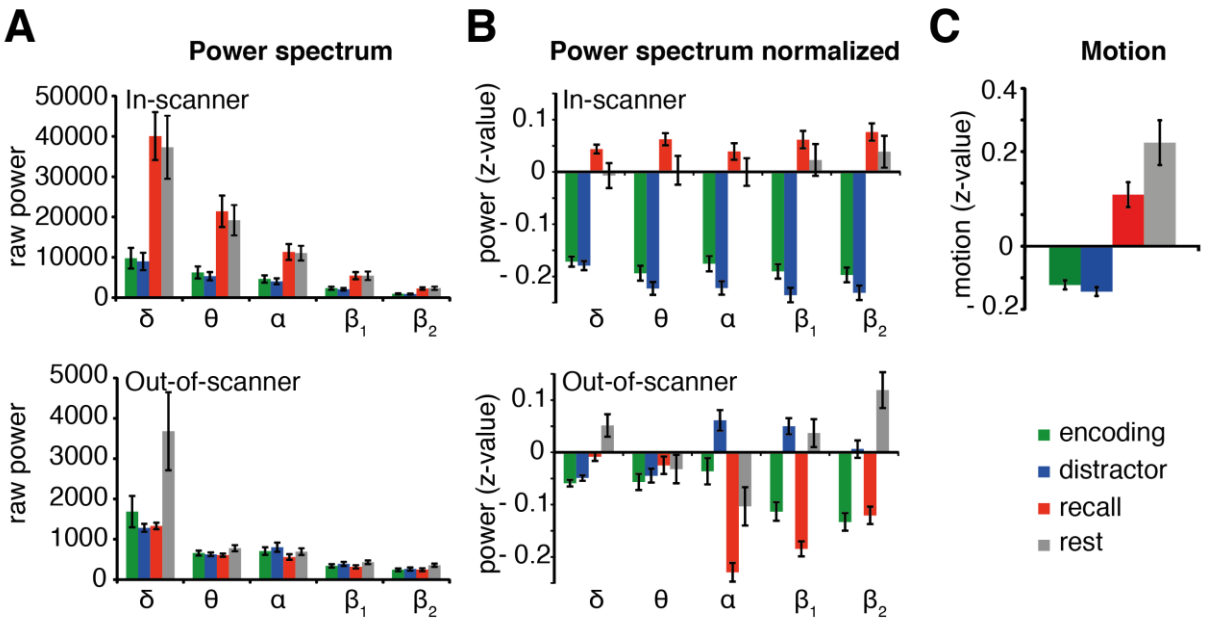

Figure 3: Mean power and motion across task phases

EEG power is highly distorted in-scanner compared with out-of-scanner. (A) Mean absolute oscillatory power across the different phases of the experiment plotted for in-scanner and out-of-scanner data. There is a remarkable difference in scaling: power of inside scanner data is 10 times higher than outside scanner data (note the order-of-magnitude difference in ordinate scales for in-scanner and out-of-scanner data). (B) Z-transformed mean power of each task phase reveal that the frequency spectrum in the out-of-scanner data varies with experimental phase whereas in-scanner data show very little variation between phases. Mean motion per condition is shown in (C) and highly resembles mean power per condition in-scanner. Error bars show SEM.

As an assessment of data quality in- and out-of-scanner, mean raw EEG power in-scanner for all task phases was contrasted with out-of-scanner data. Note the difference between in-scanner data to out-of-scanner data (see Figure 3A), especially in the lower frequencies the average power throughout the experiment is 10 times higher in-scanner compared to out-of-scanner conditions. Especially power during the high motion free recall and rest periods is drastically increased. Note also that the average power during encoding phases here reflects average power before visual artifact correction (see difference in motion before and after visual trial inspection in Figure 5). EEG power irrespective of frequency band was always highest for the rest and recall (high movement) conditions, whereas out-of-scanner data show frequency band specific variations across the task phases. This is especially apparent when controlling for the difference in scaling between measurements by normalization to the respective mean and standard deviation (Figure 3B). For example in data recorded out-of-scanner, alpha power (9-12Hz) during the distractor phase, a visual attention task, is more pronounced than during other phases. Also, during the free recall phase, when participants spoke, larger suppression of alpha and beta (9-20Hz) is evident presumably related to motor activity. In-scanner data is lacking these pronounced frequency specific effects. The differences between these two datasets show that the out-of-scanner EEG reflects general neurophysiological characteristics of the task whereas in-scanner EEG power across frequency bands and tasks seems to be largely driven by a common generator. A probable common generator is motion, as mean EEG power in-scanner across phases (Figure 3B) closely resembles average relative motion across all task phases (Figure 3C).

3.2 Task-related EEG effects: in-scanner EEG contrasted with out-of-scanner EEG

In both datasets, in- and out-of-scanner, memory-encoding effects were analyzed by contrasting power in frequency bands from 2-20 Hz depending on subsequent memory performance. This contrast of later successfully remembered and later forgotten trials is usually termed subsequent memory effect (SME; (Paller and Wagner, 2002). For in-scanner data, a sliding cluster statistic revealed only positive SMEs, i.e. higher power for later remembered than for later forgotten trials (Figure 4A). In the theta band (4-7 Hz), two clusters of positive SMEs were evident from 500 ms before until 500 ms post word

onset, and another cluster 1500 – 2500 ms after word onset (highlighted boxes and topographies in Figure 4A). Importantly, these theta SMEs in-scanner are in stark contrast to the effects found in the out-of-scanner dataset (Figure 4 B). In this dataset negative memory SMEs in the theta frequency range were found, i.e. less power for later remembered than later forgotten words. These negative SMEs were evident 500 – 1000 ms and 1500 – 2500 ms after word presentation (Figure 4B). A direct comparison of these SMEs also revealed significantly larger increases in power for in-scanner SMEs in contrast to out-of-scanner SMEs (see Figure S3). EEG data recorded outside the scanner is more reliable, i.e. free of any MR-related artifacts, and as solely the factor in/outside scanner was manipulated, the positive theta effect in-scanner is attributable to artifacts caused by the scanning environment. Notably, negative as well as positive SMEs in the theta frequency range are in line with a host of recent EEG studies (see(Hanslmayr and Staudigl, 2014)**,** for a recent review). Of note, the in-scanner theta effects seemed to be not limited to the theta frequency range but rather appeared to be part of an unselective power increase ranging from 2-20 Hz.

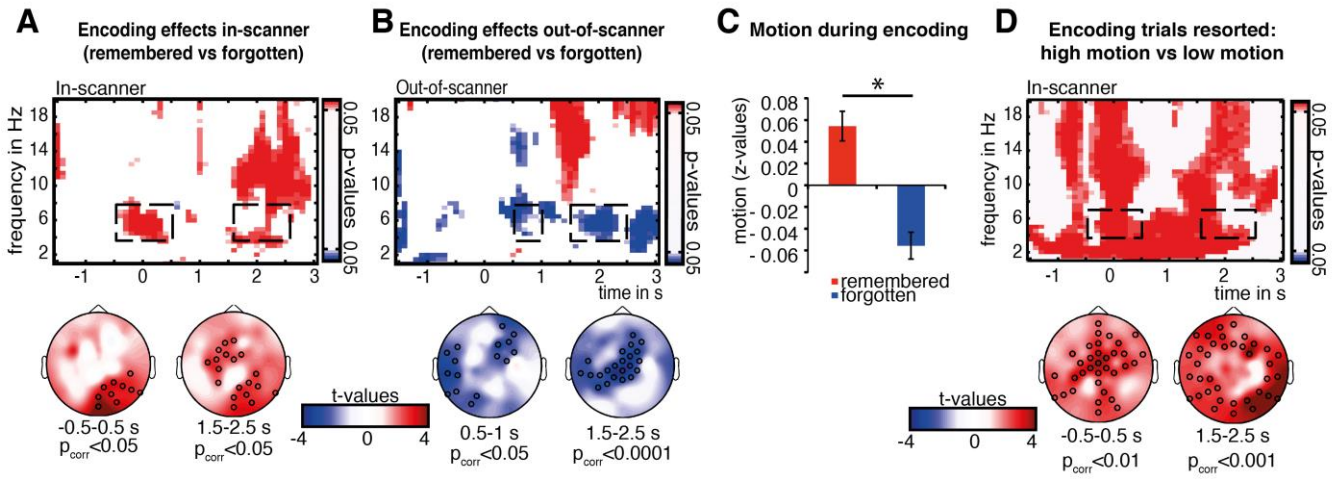

Figure 4: Memory encoding effects and motion

(A) In-scanner data showed clusters of significant positive memory encoding effects. (B) In contrast, out-of-scanner data revealed positive and negative effects. Specifically, effects in the theta frequency range (~4-7 Hz) are reversed in-scanner compared with out-of-scanner: increases in theta power were found in-scanner, whereas decreases in theta power were evident out-of scanner to be related to successful memory formation. (C) Motion was significantly higher during later remembered trials than during forgotten trials, bars plotted here show the normalized motion measure during encoding trials (D) Resorting the same trials as in (A) not regarding memory performance, but regarding motion during the trials reveals significant power increases similar as for in-scanner memory effects. Topography plots in (A), (B) and (D) show theta effects highlighted in the time-frequency plots above with grey boxes; circles highlight electrodes showing significant differences. Time-frequency plot shows p-values for time-frequency bin that reveal significant differences between remembered and forgotten trials. Warm colors indicate increases in power for remembered/high motion trials in contrast to forgotten/ low motion trials respectively. Error bars show SEM.

3.3 Small event-related motion causes spurious event-related oscillatory effects

The above analyses show that EEG power in-scanner closely tracks motion artifacts suggesting motion as potential source of the artifactual task-related theta increases. However, correlation between motion and EEG power alone cannot explain the reversal of the theta effects related to task performance (i.e. subsequent memory) between the two datasets. For motion artifacts to drive task-related contrasts, motion needs to be correlated with memory formation. Analysis of motion parameters showed that motion was indeed task related (Figure 4C). Specifically, the motion measure

during those encoding trials that passed rigorous artifact rejection was z-transformed and contrasted dependent on memory performance. Surprisingly, participants very robustly exhibited more head motion during the encoding of words that were subsequently remembered compared to forgotten words ($T(18)=4.47$ $p<0.001$). Furthermore, in line with our other findings, splitting encoding trials into high and low motion trials, regardless of memory outcome, revealed that head motion and EEG power are indeed strongly related, with high motion relative to low motion trials inducing EEG power increases, especially in lower frequency bands (Figure 4D). Additionally, the time-frequency range of high vs. low motion effects was comparable to the positive SMEs obtained in scanner (comparing Figures 4A & 4D, S3). The motion induced EEG power increases were present in all frequency bands. Especially in the theta band, this increase was continuous throughout the whole trial period (Figure 4D). Together, these analyses reveal that small task-related differences in motion can cause task-related effects in in-scanner EEG data.

3.4 Motion showing task-related differences

Event-related motion causing the spurious "subsequent-memory-effect" in each of the three translation and rotation dimensions are shown in Figure 5. Relative motion between consecutive realignment parameters are plotted to show the pattern of event- related motion in absolute mm and radians comparable to the typical realignment parameter output of fMRI preprocessing pipelines. In general, motion during encoding - even before excluding artifactual trials - was small (Figure 5A). Average motion in trials that passed visual inspection during preprocessing (Figure 5A, red and blue bars) is even lower than in trials before artifact inspection and rejection (Figure 5A, green bars) demonstrating that visual artifact correction of EEG data also implicitly reduces the magnitude of motion in the remaining data. Mean motion in each translation and rotation dimension is higher for successfully encoded trials in contrast to later forgotten trials (Figure 5A red compared with blue). To assess the statistical significance of this effect, mean motion of *z*-transformed relative motion in each motion dimension was subjected to a repeated measurement ANOVA with factors motion direction and memory. The ANOVA showed no significant interaction ($F(1,18)=1.343$), no significant main effect of motion direction ($F(1,18)=1.250$) but a significant effect of memory ($F(1,18)=6.617$; $p<0.05$)

indicating a memory effect for motion that was unspecific to any given movement direction. Albeit qualitatively the biggest memory related differences in motion were related to a *z*-translation (Figure 5A, red compared with blue). Figure 5B shows the distribution of this motion parameter (*z*-translation) for each participant and trial, which reveals that mean relative motion across all used trials and participants did not exceed 0.1 mm with the majority of movement being below 0.2 mm. This latter result shows that the task related effect was driven by movements that were small in magnitude but which consistently correlated with memory (as opposed to a few large movement outliers driving the effect). One would expect that motion increases across the recording session and that such an increase in motion across trials might explain the reported task related effect. Importantly, differences in motion between remembered and forgotten trials were not related to difference in position of the trials in the recordings. Indeed, the higher motion remembered trials tended to occur on average even earlier (M=1152 scan, std =180) than the lower motion forgotten trials (M=1199 scan, std=209), albeit this difference was not significant ($T(18)=-1.244$, $p>0.2$).

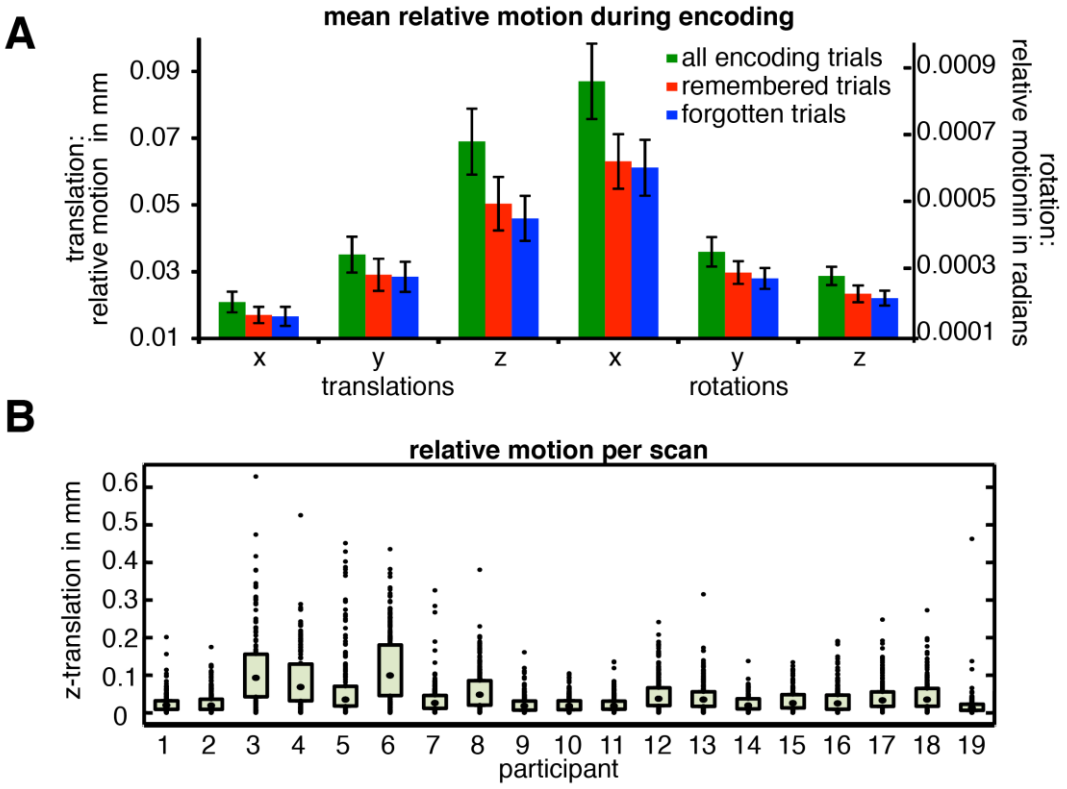

Figure 5: Overview of the relative motion during encoding

(A) shows relative motion (here: differences between realignment parameters of consecutive volumes) in all 6 motion dimensions (*x*, *y*, *z* planes for translation and rotation) during all of the encoding epochs (green bar) and for all trials used in memory effects analysis and EEG power-fMRI correlations (blue and red bars). To highlight memory related motion differences trials are split into remembered (red) and forgotten (blue) trials. (B) Distributions of relative translational motion in the *z* direction, the direction showing the largest relative movements. The median motion is highlighted in the center of the boxplots, borders of the rectangle signify the respective first and third quartile. Note that all relative motion is below 0.5 mm and all average motion is below 0.1 mm.

3.5 Motion causes spurious EEG-fMRI correlations

Next, we were interested in whether motion can also introduce spurious EEG-fMRI correlations. This is a highly relevant question given that EEG-BOLD correlations are the major motivation of most multimodal imaging studies (Hanslmayr et al., 2011; Mantini et al., 2007; Scheeringa et al., 2011). To this end EEG time courses are usually convolved with the HRF and used as predictors of fMRI time courses in a GLM. Therefore, it is important to elucidate if motion driven correlations with the fMRI

data are also evident after convolution with the HRF. To test for this possibility, BOLD signals were separately correlated with convolved EEG power and convolved motion.

In a first step, we were interested in the general pattern of convolved motion-BOLD correlations including high motion task phases, and whether EEG-BOLD correlations follow the same pattern. For this analysis theta power and motion parameters throughout the scanning session were convolved and put as regressor of interest in two separate GLMs (GLM-alltheta and GLM-allmotion). Both continuous theta power and motion regressors showed widespread negative BOLD correlations in largely overlapping areas (Figure 6A, $p<0.001$, clustersize$\geq$10, see SI Table S1), especially in regions that are known to be susceptible to artifacts, like the ventricles and areas on tissue borders. However, strong negative correlations were also obtained in regions relevant to cognitive processes: medial frontal, medial- and lateral-parietal regions. This demonstrates that convolved EEG power and convolved motion indeed correlate with fMRI and that these correlations largely overlap.

These first BOLD-motion/EEG correlations identified similarities between motion and EEG correlations. However, including highly artifact loaded data (i.e. EEG data during the recall phase) does not resemble typical analysis pipelines. A more relevant question thus is if motion can also produce spurious correlations after stringent, state-of-the-art removal of data containing artifacts. A second set of GLMs was constructed to explore if the impact of motion on EEG and BOLD signals is large enough to also drive theta-BOLD correlation when using a standard analysis pipeline. A theta GLM (GLM-cleantheta) was designed, including only convolved theta power of encoding trials that survived rigorous artifact removal. To further control for movement related artifacts, realignment parameters were added to the GLM-cleantheta. Matching this more conservative approach of correlating theta and BOLD signal, a second motion GLM was setup to investigate the correlation of small movements with the BOLD signal (GLM-smallmotion, only including motion not exceeding 0.2mm in any of the translational dimensions throughout the scanning session). The results of this analysis still revealed a similar motion driven pattern as the previous analysis (Figure 6B, Table S4). Theta power during encoding still correlated negatively with BOLD signal predominantly at medial locations (cyan areas, Figure 6B, $p<0.001$, clustersize$\geq$10), areas that also show a strong overlap with areas correlating with motion (Figure 6B, white areas). Lowering the statistical threshold to $p<0.005$

reveals that theta-BOLD correlations show a rim structure at frontal coronal slices and in axial slices (Figure 6B green areas) and exhibit larger overlap with motion-correlated areas (Figure 6B, yellow and white areas). Importantly, the correlations shown in green and cyan could easily pass as physiologically plausible correlates of medial frontal theta power (Cohen, 2014). Clusters showing positive correlations between motion and BOLD signals, and theta and BOLD signals, are reported in Figure S3B. These positive correlations were predominantly found in areas related to voluntary movements such as the precentral gyrus and the cerebellum.

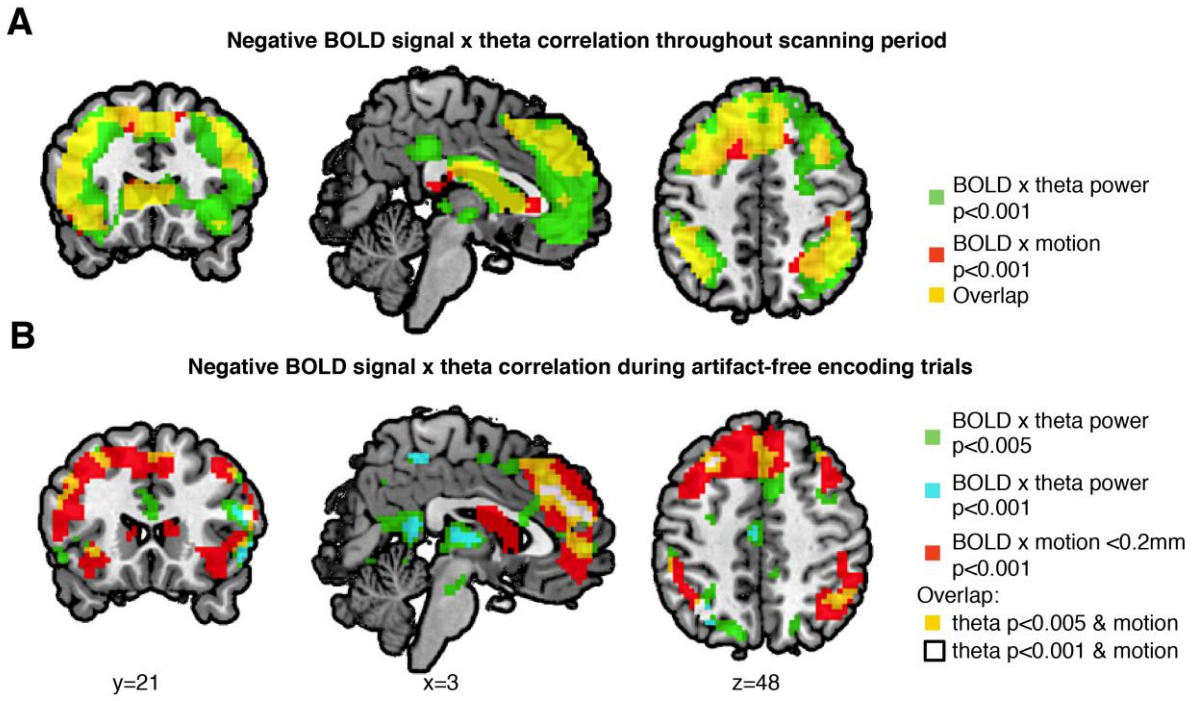

Figure 6: Negative EEG-BOLD signal and negative motion-BOLD signal correlations. Correlating convolved continuous theta power throughout the scanning session resulted in large overlap with areas correlating with convolved motion parameters throughout the recording, including high motion periods (A). Areas shown in green are significantly negatively correlated with theta power and areas shown in red are significantly negatively correlated with convolved motion regressor, areas in yellow indicate the overlap of these effects. (B) Correlations of convolved continuous theta power restricted to encoding phase trials (different statistical thresholds in cyan and green, respectively) that passed artifact correction still showed an overlap (yellow) with areas exhibiting significant correlation with small movements (red). See figure S4 for unconvolved EEG-BOLD correlations, alpha/beta band EEG-BOLD correlations, and positive EEG/motion BOLD correlations.

Above we show that power across all frequency bands (<20 Hz) correlates with motion, therefore similar power-BOLD correlations were expected for alpha (8-12 Hz) and beta (13-20 Hz) frequency ranges. Accordingly, a GLM-cleanalpha and a GLM-cleanbeta were set up, matching the GLM-cleantheta. Indeed, the results of this analysis resembled the correlation patterns obtained for theta (see Figure S4, Table S3). Further control analyses investigated the nature of the motion/power correlations by comparing models with convolved regressors to results of non-convolved models (Figure S4 C&D, Table S4 & S5). These models reveal that correlations with non-convolved regressors, including periods of large movements, match and exceed correlations with convolved regressors. This observation suggests that correlations observed with convolved regressors are, at least in part, due to a prolonged motion artifact. Likely spin history effects, induced during large movements cause a prolonged signal change in the EPI data mimicking a BOLD signal change in the GLM with the convolved regressors (see Figure S4C). During small motion however, stronger correlations were found in convolved models, suggesting that correlation of power during small motion periods is only partially, if at all, linked to spin history MR motion related artifacts, but is instead related to neural activity that correlates with motion or physiological vascular correlates of motion (Bright et al., 2015), see Figure S4D, Table S5). Note that the reported EEG-BOLD correlations and motion-BOLD correlations were calculated after orthogonalizing the motion/EEG regressors to the task regressor. Therefore the EEG-BOLD or motion-BOLD effects are likely not related to shared variance between the task and EEG/motion (see (Eichele et al., 2005; Scheeringa et al., 2009)).

Finally, to demonstrate that the reported correlations are due to specific time-locked motion-BOLD and EEG power-BOLD correlations, as opposed to unspecific differences in motion or power, null models were set up resembling GLM-allmotion and GLM-alltheta with a randomized theta power and motion parameters time series convolved with the HRF. In these null models, no cluster exceeded a $p<0.001$, clustersize$\geq$10 threshold.

4 Discussion

This study demonstrates that movement related artifacts in simultaneous EEG-fMRI induce spurious effects in EEG data, but also spurious EEG-BOLD correlations. Movement in the MR scanner is positively correlated with amplitude increases in simultaneously recorded EEG, even during low motion epochs. This tight relationship between movement and EEG results in motion causing spurious EEG-fMRI effects in a twofold manner: in the magnetic field of the scanner, tiny differences in event-related motion between task conditions can (i) produce spurious task-related effects in EEG data that can be in stark contrast to task-related effects out-of-scanner, and (ii) elicit spurious EEG-BOLD correlations by introducing motion-related artifacts concurrently in EEG and fMRI data.

In our case, small task correlated differences in motion during a memory task introduced artifacts strong enough to reverse memory related theta effects that were observed for this task out-side the scanner (Figure 4). Furthermore, convolving theta power with an HRF before correlating it with the measured BOLD series, an analysis commonly carried out to reveal mutual generators of hemodynamic fMRI effects and electrophysiological oscillatory effects, exhibited results closely matching correlations of motion with BOLD signals. In the presence of even only small motion in the data, EEG-BOLD correlations do thus not reveal neural activity related to brain oscillatory power, but exhibit motion related changes present in EEG and fMRI. Importantly, these motion driven EEG-BOLD correlations were obtained using a standard analysis pipeline after convolving time courses with the HRF, employing motion correction, and without exceedingly high motion in the data (mean relative motion below 0.05 mm, see Figure 5).

4.1 Motion causes seemingly neurophysiological plausible effects using common analysis steps

Alarmingly, the presented pattern of spurious motion related EEG-BOLD effects was found employing preprocessing steps and analysis steps commonly employed in EEG-fMRI (Baumeister et al., 2014; de Munck et al., 2007; de Munck et al., 2009; Debener et al., 2007; Hanslmayr et al., 2013; Hanslmayr et al., 2011; Jann et al., 2009; Jansen et al., 2012; Laufs et al., 2006b; Laufs et al., 2003; Li et al., 2012; Liu et al., 2012b; Mayhew et al., 2010; Mayhew et al., 2012; Mayhew et al., 2013; Meyer et al., 2013; Novitskiy et al., 2011; Plichta et al., 2013; Regenbogen et al., 2012; White et al., 2013)

and could easily pass as neurophysiological plausible results. The relationship of theta oscillatory power and successful memory formation remains controversial, as opposing effects have been reported by recent studies (Hanslmayr and Staudigl, 2014). Only artifact free, out-of-scanner control data rendered the in-scanner theta effects and fMRI correlations implausible, and prompted us to conduct an in-depth analysis of motion during scanning which revealed the cause of this spurious theta power increase. BOLD-motion/power correlations were significant in areas typically thought to exhibit motion effects such as ventricles, regions at the rim of the cortex, but also in parietal cortex and in midline regions (Lemieux et al., 2007) (Figure 6). The spurious correlations between theta power and frontal midline regions we report do, however, fit with the hypothesis of medial frontal cortex generating theta oscillations (Cohen, 2014), which could easily lead to misinterpretation of our data. Several published simultaneous EEG-fMRI studies investigating correlations of theta power and BOLD signals have reported similar negative correlations in frontal midline regions (Sammer et al., 2007; Scheeringa et al., 2009; White et al., 2013). The pattern of negative correlations of low frequency power with BOLD signals in several cortical areas, reported here, would also be in line with prior work suggesting a negative relationship of low frequency power and BOLD signals (Hermes et al., 2014; Mukamel et al., 2005; Zumer et al., 2014). This resemblance of spurious correlations with physiologically expected effects is a serious problem for simultaneous EEG-fMRI studies trying to unravel the relationship of BOLD signals and electrophysiological activity. Even when assuming the presence of "real" EEG-BOLD correlations in the data, the overlap of motion and EEG BOLD correlations renders true and spurious effects indistinguishable.

Even very small movements, generally not considered problematic in fMRI studies, correlate positively with increases in EEG amplitudes. During the encoding phase, task-related average motion differences smaller than 0.01mm between successfully encoded trials in contrast to forgotten trials (see Figure 5) caused spurious task related EEG power increases, rather than the expected decreases from data recorded out-side the scanner (Figure 4B). The fact that motion effects cause completely opposing task related EEG effects in the data shown here, is likely to be an extreme example of motion dominating the effect of interest, although a similar less extreme observation has previously been reported, see Debener et al. (2005). Direct comparisons of in-scanner and out-of-scanner EEG data are

rarely reported. When they are reported EEG features are commonly altered, such as the reduction of EEG power amplitudes reported by Scheeringa et al. (2009) at the channel level. Changes between in and out-of-scanner data might be attributable to non-randomly distributed motion artifacts.

4.2 Task related motion causing event related effects

An open question is: What kind of motion caused this effect in the current data? The very small magnitude of the motion during the encoding phase indicates that these effects might rather be related to physiological motion than voluntary head movements. Negative EEG-BOLD correlations even exceeded the negative motion-BOLD correlations in t-values and spatial extent, demonstrating that EEG can provide a more sensitive motion measure than the realignment parameters (Zotev et al., 2012). Realignment parameters are considered to provide a very high spatial resolution up to 100 µm (Friston et al., 1996). However, they possess a very low temporal resolution (in the present case 2 seconds). Consequently, the combined motion measure as a derivative of the realignment parameter is insensitive to rapid, periodical movements, which would still produce artifactual increases in EEG power. Such a rapid, periodical movement for example is caused during each heartbeat, as each heartbeat causes a small nodding movement with velocities up to 0.5 mm per second (Mullinger et al., 2013).

This capacity of EEG to capture physiological motion of very small magnitude links the presented results to research focusing on the influence of physiological measures on fMRI. Several studies have shown that physiological noise related to respiration and heart-rate variability correlates with cognitive tasks (Birn et al., 1999; Birn et al., 2009; Ent et al., 2014; Park et al., 2014; Vlemincx et al., 2011) and elicits prolonged negative correlations with BOLD signals - especially in midline areas (Birn et al., 2009; de Munck et al., 2008; Ent et al., 2014; Shmueli et al., 2007). Furthermore, task related changes in physiology can produce BOLD signal changes in vascular networks mimicking neuronal network activations (Bright et al., 2015). Note that in the present study no difference in the distribution of detected heartbeats depending on task performance was found (Figure S5), therefore task related spurious EEG effects are not related to changes in heartbeat distributions across trials. However spurious EEG-BOLD correlations might still be related to heartbeat related artifacts. An

fMRI study focused on memory encoding, similar to the present study, showed that respiration is phase-locked to item presentation (Huijbers et al., 2014). This respiration phase-locking was stronger for later remembered in contrast to later forgotten items. Interestingly, respiration also predominantly correlates with BOLD effects in midline regions (Birn et al., 2006; Huijbers et al., 2014), resembling the spatial pattern of motion-related correlations in the present results. Our results show that such small physiological motion, which in event related fMRI does not cause spurious activation (Birn et al., 1999), can dramatically drive effects in simultaneous EEG-fMRI. Future research needs to investigate respiration and other physiological measures (e.g. end-tidal CO_2) and measure head motion directly to reveal the source of these movements, thus inspiring development of methods to control for these artifacts.

4.3 Motion/EEG-BOLD correlations overlap after convolving motion and EEG with the HRF

At first glance it is surprising that negative motion-BOLD/EEG-BOLD correlations were obtained after convolving with the canonical HRF. Correlations of convolved motion with BOLD signals have been rarely reported (however, see (Jansen et al., 2012)). Commonly, one would expect that motion related artifacts immediately affect BOLD signals, and therefore motion artifacts would be omitted by effectively delaying the response ~5sec by convolving the motion time course with the HRF. However, the effects of large motion are indeed prolonged enough to exhibit a similar, albeit weaker, correlation with BOLD signal after convolution. Negative correlations of non-convolved large motion shown in the supporting material (Figure S4C) reveal similar effects as after convolution in typical motion artifact prone regions. Similar widespread artifactual negative correlations between head motion and fMRI have consistently been found (Satterthwaite et al., 2013; Yan et al., 2013), and motion can induce artifacts lasting up to 10 sec (Power et al., 2014). Convolving power time series therefore does not prevent motion driven spurious correlations.

Correlations of convolved power and motion seem not only to be related to motion artifacts but are also found in regions involved in planning and executing motion like the motor cortices and the cerebellum. Those regions exhibit mainly positive correlations and in contrast to the motion artifacts are only evident after convolution (Figure S4B) and may reflect neural origins of motion, as

previously suggested (Yan et al., 2013). Another striking pattern, which emerges especially when correlating power or motion during low movement phases, is an apparent resemblance with resting state networks (Fox and Raichle, 2007). Negative correlations with resting state networks might arise because lower motion periods could indicate periods of low task involvement and consequently decreases in motion might indicate increases in resting state activity. Therefore, some of the convolved motion-BOLD correlations might indeed be related to real neural activity. However, this neural activity is still linked to motion rather than the desired task-related EEG changes, which further complicates separating real EEG-BOLD correlations from motion driven EEG-BOLD correlations. Importantly, the correlation between EEG/motion and BOLD signal cannot be explained by changes in task related BOLD activity. The overlap between the areas showing significant activation related to memory formation (e.g. changes in activity for remembered vs. forgotten) and the theta regressor were relatively small (5.5/2.6% overlap between neg/pos SME and negative theta respectively). Also no memory related changes in frontal midline activity were observed. This suggests that EEG-BOLD correlations indeed reflect motion related activity, in part driven by motion artifacts and in part motion related changes in neural activity.

An alternative explanation is that these network regions are also prone to exhibit cardiorespiratory related correlations (Birn et al., 2006; Shmueli et al., 2007; van Buuren et al., 2009). Therefore, EEG as a very sensitive measure of voluntary and physiological motion in a magnetic field could reveal similar correlations with the default mode network as cardiorespiratory measures. Together, our reported EEG-BOLD correlations seem to be more directly connected to motion and not to cortical activity connected to brain oscillatory responses. We hypothesize that when large movements are present, the correlations that we observe are primarily driven by voluntary movements (e.g. speech) causing MRI artifacts, such as spin history effects, as significant correlations are observed in wide-spread areas without convolution of the EEG/motion regressor with the HRF. However, when only small movements are present we suggest the primary driver of the correlations that we observe are physiological in origin, i.e. related to changes in respiration with task, since little correlation is observed without convolution with the HRF.

4.4 Impact of motion on simultaneous EEG-fMRI studies

The relationship between motion and EEG power might explain the lack of distinct correlation patterns found between specific frequency bands and BOLD responses (de Munck et al., 2009; Lavallee et al., 2014; Mantini et al., 2007), the lack of correlation of oscillatory EEG power in task-active regions (Ritter et al., 2009; Scheeringa et al., 2009), and the high variability in correlation patterns across participants (de Munck et al., 2007; de Munck et al., 2009; Goncalves et al., 2006; Laufs et al., 2006a; Meyer et al., 2013). In particular, we suggest that EEG-fMRI studies investigating the relationship between oscillatory EEG power and BOLD responses in resting state are particularly susceptible to spurious correlations, since in resting state studies, continuous power time series are typically correlated with BOLD time series similar to the analysis presented here. In contrast, the common approach of including trial-based average power as a task-specific parametric modulator in the fMRI model (Debener et al., 2006; Hanslmayr et al., 2011; Scheeringa et al., 2009; Zumer et al., 2014) could reduce the impact of motion as long as motion is not task correlated. Therefore one important implication of our results is to avoid correlations of EEG power with fMRI data unless there is evidence that the EEG power measures are not related to movement.

Motion in simultaneous EEG-fMRI recordings also impacts on the success of the gradient and BCG artifact correction, which is an additional undesirable impact of motion on data quality. Specifically, movement changes the shape and amplitude of the gradient and BCG artifacts in EEG because of the changed position of electrodes in the magnetic field. Consequently, artifact templates do not explain the individual artifact occurrences well, resulting in a less accurate correction (see Figure S6). Increased residual BCG artifacts caused by motion can, at least in part, explain the prolonged increases in the theta frequency activity during high motion trials (Figure 4D, see also Figure S6), as the BCG artifact shows highest amplitudes in the theta frequency range (LeVan et al., 2013). The OBS method used in this study (Niazy et al., 2005) allows for temporal variations in BCG artifact by fitting an optimal basis set to the data, but still assumes spatial stationarity. Average artifact subtraction methods that are widely used are theoretically even less adapted to account for variability in artifacts**.** Considering motion in-scanner might therefore also be the key to improve gradient and BCG artifact correction**.**

4.5 Possiblities to correct for motion artefacts in simultaneously recorded EEG

Correlating continuous EEG and fMRI measures is difficult to avoid when investigating ongoing effects, and can provide high power to detect effects of interest. An interesting solution to control for motion on EEG-fMRI data is to record motion co-registered to EEG recordings with a sufficiently high sampling rate. Recently, several motion-recording approaches have been proposed (Abbott et al., 2014; Chowdhury et al., 2014; Jorge et al., 2015; LeVan et al., 2013; van der Meer et al., 2015). Accurate measurement of electrode positions and wire paths in combination with high resolved movement measures might be the key to fully understand the impact of motion on simultaneously recorded EEG (Yan et al., 2009; Yan et al., 2010). Currently none of these methods are used in standard EEG-fMRI setups or are validated in measurements of oscillatory activity during cognitive tasks. Using such techniques will likely improve the validity of EEG-fMRI results and might be the key to establishing EEG-fMRI as a more widely used neuroimaging method.

Post-processing methods already available may also be of some help in addressing this problem. Some studies have concentrated on a single ICA component of interest to de-noise the data (Debener et al., 2005; Eichele et al., 2005; Scheeringa et al., 2011; Scheeringa et al., 2009). However this approach constrains the research questions that can be addressed by simultaneous EEG-fMRI quite a bit, as only processes that reliably map onto specific ICs, i.e. posterior alpha activity or the error related negativity, can be investigated. ICA as a blind source separation algorithm that heavily relies on the spatial stationarity of the data is also limited in its ability to remove motion artifacts from the data (see Figure S2 and (Debener et al., 2007; Jorge et al., 2015)). One potentially powerful, however not yet commonly used de-noising strategy is beamforming, as separating spatial sources of the EEG signal is an efficient artifact removal strategy (Brookes et al., 2009a; Zumer et al., 2014). This approach has the advantage for motion correction by not assuming spatially stationary sources, unlike ICA approaches, but does not lend itself to analysis of all types of EEG data (Brookes et al., 2009b).

An approach that has been used for EEG-fMRI analysis is to remove outliers from the EEG power time series (Sadaghiani et al., 2010; Scheeringa et al., 2009; Yuan et al., 2013) from any regressor created. However, these studies set quite liberal thresholds for outlier removal of 4 or 5 standard deviations above the mean, which is not effective to prevent correlations with motion (Figure

2). Outliers can also be determined by applying a threshold to data on the basis of realignment parameters. For instance, one of the first EEG-fMRI studies correlating continuous alpha power with BOLD changes excluded all scans with motion exceeding a threshold of one standard deviation above the mean (Goldman et al., 2002). A similar approach of censoring motion scans has been demonstrated as a useful approach in resting state fMRI studies (Power et al., 2014) and event related fMRI designs (Siegel et al., 2014). Our results suggest this is not stringent enough when considering EEG-BOLD signal correlations when motion may be correlated with the task due to anything from voluntary movements to a change in breathing. Despite all potential clean up techniques the gold standard to validate EEG effects obtained in the scanner is still contrasting in-scanner EEG data with data recorded outside of scanner. Only the comparison of in-and out-of-scanner effects yields a transparent check of the in-scanner data quality. This is especially important for the low frequency range up to 20 Hz, in which motion and other artifacts are most pronounced during simultaneous recordings (Masterton et al., 2007).

5 Conclusion

Simultaneous EEG-fMRI undoubtedly is a highly useful research tool, which could provide important insights into countless research questions. However, poor data quality of simultaneously recorded EEG, especially due to motion induced artifacts, is still a major limitation for simultaneous EEG-fMRI studies. Preventing motion and controlling results for motion is therefore an important step in acquiring valid results. Artifacts related to small head and physiological motion that would be negligible in each modality alone cause spurious results that are difficult to separate from real neurophysiological effects. Tools to record motion in the scanner, and artifact correction methods incorporating those measures, might be the key to reliable EEG-fMRI correlations in future studies.

Acknowledgments

The research presented in this work was supported by a grant from the Deutsche Forschungsgemeinschaft (Project HA 5622/1-1) awarded to Simon Hanslmayr.

References

Abbott, D.F., Masterton, R.A., Archer, J.S., Fleming, S.W., Warren, A.E., Jackson, G.D., 2014. Constructing Carbon Fiber Motion-Detection Loops for Simultaneous EEG-fMRI. Front Neurol 5, 260.

Allen, P.J., Polizzi, G., Krakow, K., Fish, D.R., Lemieux, L., 1998. Identification of EEG events in the MR scanner: the problem of pulse artifact and a method for its subtraction. Neuroimage 8, 229-239.

Baumeister, S., Hohmann, S., Wolf, I., Plichta, M.M., Rechtsteiner, S., Zangl, M., Ruf, M., Holz, N., Boecker, R., Meyer-Lindenberg, A., Holtmann, M., Laucht, M., Banaschewski, T., Brandeis, D., 2014. Sequential inhibitory control processes assessed through simultaneous EEG-fMRI. Neuroimage 94, 349-359.

Birn, R.M., Bandettini, P.A., Cox, R.W., Shaker, R., 1999. Event-related fMRI of tasks involving brief motion. Hum Brain Mapp 7, 106-114.

Birn, R.M., Diamond, J.B., Smith, M.A., Bandettini, P.A., 2006. Separating respiratory-variation-related fluctuations from neuronal-activity-related fluctuations in fMRI. Neuroimage 31, 1536-1548.

Birn, R.M., Murphy, K., Handwerker, D.A., Bandettini, P.A., 2009. fMRI in the presence of task-correlated breathing variations. Neuroimage 47, 1092-1104.

Bright, M.G., Whittaker, J., Driver, I., Murphy, K., 2015. Task-correlated physiology reveals vascular-neural networks. Proc. Intl. Soc. Mag. Reson. Med. 23.

Brookes, M.J., Vrba, J., Mullinger, K.J., Geirsdottir, G.B., Yan, W.X., Stevenson, C.M., Bowtell, R., Morris, P.G., 2009a. Source localisation in concurrent EEG/fMRI: applications at 7T. Neuroimage 45, 440-452.

Brookes, M.J., Vrba, J., Mullinger, K.J., Geirsdóttir, G.B., Yan, W.X., Stevenson, C.M., Bowtell, R., Morris, P.G., 2009b. Source localisation in concurrent EEG/fMRI: applications at 7T. Neuroimage 45, 440-452.

Chowdhury, M.E., Mullinger, K.J., Glover, P., Bowtell, R., 2014. Reference layer artefact subtraction (RLAS): a novel method of minimizing EEG artefacts during simultaneous fMRI. Neuroimage 84, 307-319.

Cohen, M.X., 2014. A neural microcircuit for cognitive conflict detection and signaling. Trends Neurosci 37, 480-490.

de Munck, J.C., Goncalves, S.I., Faes, T.J., Kuijer, J.P., Pouwels, P.J., Heethaar, R.M., Lopes da Silva, F.H., 2008. A study of the brain's resting state based on alpha band power, heart rate and fMRI. Neuroimage 42, 112-121.

de Munck, J.C., Goncalves, S.I., Huijboom, L., Kuijer, J.P., Pouwels, P.J., Heethaar, R.M., Lopes da Silva, F.H., 2007. The hemodynamic response of the alpha rhythm: an EEG/fMRI study. Neuroimage 35, 1142-1151.

de Munck, J.C., Goncalves, S.I., Mammoliti, R., Heethaar, R.M., Lopes da Silva, F.H., 2009. Interactions between different EEG frequency bands and their effect on alpha-fMRI correlations. Neuroimage 47, 69-76.

Debener, S., Mullinger, K.J., Niazy, R.K., Bowtell, R.W., 2008. Properties of the ballistocardiogram artefact as revealed by EEG recordings at 1.5, 3 and 7 T static magnetic field strength. Int J Psychophysiol 67, 189-199.

Debener, S., Strobel, A., Sorger, B., Peters, J., Kranczioch, C., Engel, A.K., Goebel, R., 2007. Improved quality of auditory event-related potentials recorded simultaneously with 3-T fMRI: removal of the ballistocardiogram artefact. Neuroimage 34, 587-597.

Debener, S., Ullsperger, M., Siegel, M., Engel, A.K., 2006. Single-trial EEG-fMRI reveals the dynamics of cognitive function. Trends Cogn Sci 10, 558-563.

Debener, S., Ullsperger, M., Siegel, M., Fiehler, K., von Cramon, D.Y., Engel, A.K., 2005. Trial-by-trial coupling of concurrent electroencephalogram and functional magnetic resonance imaging identifies the dynamics of performance monitoring. J Neurosci 25, 11730-11737.

Eichele, T., Specht, K., Moosmann, M., Jongsma, M.L., Quiroga, R.Q., Nordby, H., Hugdahl, K., 2005. Assessing the spatiotemporal evolution of neuronal activation with single-trial event-related potentials and functional MRI. Proc Natl Acad Sci U S A 102, 17798-17803.

Ent, D.v.t., Braber, A.d., Rotgans, E., Geus, E.J.C.d., Munck, J.C.d., 2014. The use of fMRI to detect neural responses to cognitive interference and planning: evidence for a contribution of task related changes in heart rate? Journal of Neuroscience Methods 229, 97-107.

Fox, M.D., Raichle, M.E., 2007. Spontaneous fluctuations in brain activity observed with functional magnetic resonance imaging. Nat Rev Neurosci 8, 700-711.

Friston, K.J., Williams, S., Howard, R., Frackowiak, R.S., Turner, R., 1996. Movement-related effects in fMRI time-series. Magn Reson Med 35, 346-355.

Goldman, R.I., Stern, J.M., Engel, J., Jr., Cohen, M.S., 2002. Simultaneous EEG and fMRI of the alpha rhythm. Neuroreport 13, 2487-2492.

Goncalves, S.I., de Munck, J.C., Pouwels, P.J., Schoonhoven, R., Kuijer, J.P., Maurits, N.M., Hoogduin, J.M., Van Someren, E.J., Heethaar, R.M., Lopes da Silva, F.H., 2006. Correlating the alpha rhythm to BOLD using simultaneous EEG/fMRI: inter-subject variability. Neuroimage 30, 203-213.

Hanslmayr, S., Staudigl, T., 2014. How brain oscillations form memories--a processing based perspective on oscillatory subsequent memory effects. Neuroimage 85 Pt 2, 648-655.

Hanslmayr, S., Volberg, G., Wimber, M., Dalal, S.S., Greenlee, M.W., 2013. Prestimulus oscillatory phase at 7 Hz gates cortical information flow and visual perception. Curr Biol 23, 2273-2278.

Hanslmayr, S., Volberg, G., Wimber, M., Raabe, M., Greenlee, M.W., Bauml, K.H., 2011. The relationship between brain oscillations and BOLD signal during memory formation: a combined EEG-fMRI study. J Neurosci 31, 15674-15680.

Hermes, D., Miller, K.J., Vansteensel, M.J., Edwards, E., Ferrier, C.H., Bleichner, M.G., van Rijen, P.C., Aarnoutse, E.J., Ramsey, N.F., 2014. Cortical theta wanes for language. Neuroimage 85 Pt 2, 738-748.

Huijbers, W., Pennartz, C.M., Beldzik, E., Domagalik, A., Vinck, M., Hofman, W.F., Cabeza, R., Daselaar, S.M., 2014. Respiration phase-locks to fast stimulus presentations: implications for the interpretation of posterior midline "deactivations". Hum Brain Mapp 35, 4932-4943.

Huster, R.J., Debener, S., Eichele, T., Herrmann, C.S., 2012. Methods for simultaneous EEG-fMRI: an introductory review. J Neurosci 32, 6053-6060.

Jann, K., Dierks, T., Boesch, C., Kottlow, M., Strik, W., Koenig, T., 2009. BOLD correlates of EEG alpha phase-locking and the fMRI default mode network. Neuroimage 45.

Jansen, M., White, T.P., Mullinger, K.J., Liddle, E.B., Gowland, P.A., Francis, S.T., Bowtell, R., Liddle, P.F., 2012. Motion-related artefacts in EEG predict neuronally plausible patterns of activation in fMRI data. Neuroimage 59, 261-270.

Jorge, J., Grouiller, F., Gruetter, R., van der Zwaag, W., Figueiredo, P., 2015. Towards high-quality simultaneous EEG-fMRI at 7T: Detection and reduction of EEG artifacts due to head motion. Neuroimage 120, 143-153.

Kim, H., 2011. Neural activity that predicts subsequent memory and forgetting: a meta-analysis of 74 fMRI studies. Neuroimage 54, 2446-2461.

Laufs, H., Holt, J.L., Elfont, R., Krams, M., Paul, J.S., Krakow, K., Kleinschmidt, A., 2006a. Where the BOLD signal goes when alpha EEG leaves. Neuroimage 31, 1408-1418.

Laufs, H., John, L.H., Robert, E., Michael, K., Joseph, S.P., Krakow, K., Kleinschmidt, A., 2006b. Where the BOLD signal goes when alpha EEG leaves. Neuroimage 31, 1408-1418.

Laufs, H., Kleinschmidt, A., Beyerle, A., Eger, E., Salek-Haddadi, A., Preibisch, C., Krakow, K., 2003. EEG-correlated fMRI of human alpha activity. Neuroimage 19, 1463-1476.

Lavallee, C.F., Herrmann, C.S., Weerda, R., Huster, R.J., 2014. Stimulus-response mappings shape inhibition processes: a combined EEG-fMRI study of contextual stopping. PLoS One 9, e96159.

Lemieux, L., Salek-Haddadi, A., Lund, T.E., Laufs, H., Carmichael, D., 2007. Modelling large motion events in fMRI studies of patients with epilepsy. Magn Reson Imaging 25, 894-901.

LeVan, P., Maclaren, J., Herbst, M., Sostheim, R., Zaitsev, M., Hennig, J., 2013. Ballistocardiographic artifact removal from simultaneous EEG-fMRI using an optical motion-tracking system. Neuroimage 75, 1-11.

Li, S., Mayhew, S.D., Kourtzi, Z., 2012. Learning shapes spatiotemporal brain patterns for flexible categorical decisions. Cerebral cortex (New York, N.Y. : 1991) 22, 2322-2335.

Liu, Z., de Zwart, J.A., van Gelderen, P., Kuo, L.W., Duyn, J.H., 2012a. Statistical feature extraction for artifact removal from concurrent fMRI-EEG recordings. Neuroimage 59, 2073-2087.

Liu, Z., de Zwart, J.A., Yao, B., van Gelderen, P., Kuo, L.W., Duyn, J.H., 2012b. Finding thalamic BOLD correlates to posterior alpha EEG. Neuroimage 63, 1060-1069.

Mantini, D., Perrucci, M.G., Del Gratta, C., Romani, G.L., Corbetta, M., 2007. Electrophysiological signatures of resting state networks in the human brain. Proc Natl Acad Sci U S A 104, 13170-13175.

Maris, E., Oostenveld, R., 2007. Nonparametric statistical testing of EEG- and MEG-data. J Neurosci Methods 164, 177-190.

Masterton, R.A., Abbott, D.F., Fleming, S.W., Jackson, G.D., 2007. Measurement and reduction of motion and ballistocardiogram artefacts from simultaneous EEG and fMRI recordings. Neuroimage 37, 202-211.

Mayhew, S.D., Dirckx, S.G., Niazy, R.K., Iannetti, G.D., Wise, R.G., 2010. EEG signatures of auditory activity correlate with simultaneously recorded fMRI responses in humans. Neuroimage 49, 849-864.

Mayhew, S.D., Li, S., Kourtzi, Z., 2012. Learning acts on distinct processes for visual form perception in the human brain. J Neurosci 32, 775-786.

Mayhew, S.D., Ostwald, D., Porcaro, C., Bagshaw, A.P., 2013. Spontaneous EEG alpha oscillation interacts with positive and negative BOLD responses in the visual-auditory cortices and default-mode network. Neuroimage 76, 362-372.

Meyer, M.C., van Oort, E.S., Barth, M., 2013. Electrophysiological correlation patterns of resting state networks in single subjects: a combined EEG-fMRI study. Brain Topogr 26, 98-109.

Mukamel, R., Gelbard, H., Arieli, A., Hasson, U., Fried, I., Malach, R., 2005. Coupling between neuronal firing, field potentials, and FMRI in human auditory cortex. Science 309, 951-954.

Mullinger, K.J., Havenhand, J., Bowtell, R., 2013. Identifying the sources of the pulse artefact in EEG recordings made inside an MR scanner. Neuroimage 71, 75-83.

Murphy, K., Birn, R.M., Bandettini, P.A., 2013. Resting-state fMRI confounds and cleanup. Neuroimage 80, 349-359.

Niazy, R.K., Beckmann, C.F., Iannetti, G.D., Brady, J.M., Smith, S.M., 2005. Removal of FMRI environment artifacts from EEG data using optimal basis sets. Neuroimage 28, 720-737.

Novitskiy, N., Ramautar, J.R., Vanderperren, K., Vos, D.M., Mennes, M., Mijovic, B., Vanrumste, B., Stiers, P., den Bergh, V.B., Lagae, L., Sunaert, S., Huffel, V.S., Wagemans, J., 2011. The BOLD correlates of the visual P1 and N1 in single-trial analysis of simultaneous EEG-fMRI recordings during a spatial detection task. Neuroimage 54.

Oostenveld, R., Fries, P., Maris, E., Schoffelen, J.M., 2011. FieldTrip: Open source software for advanced analysis of MEG, EEG, and invasive electrophysiological data. Comput Intell Neurosci 2011, 156869.

Paller, K.A., Wagner, A.D., 2002. Observing the transformation of experience into memory. Trends in Cognitive Sciences 6, 93-102.

Park, H.D., Correia, S., Ducorps, A., Tallon-Baudry, C., 2014. Spontaneous fluctuations in neural responses to heartbeats predict visual detection. Nat Neurosci 17, 612-618.

Plichta, M.M., Wolf, I., Hohmann, S., Baumeister, S., Boecker, R., Schwarz, A.J., Zangl, M., Mier, D., Diener, C., Meyer, P., 2013. Simultaneous EEG and fMRI reveals a causally connected subcortical-cortical network during reward anticipation. The Journal of Neuroscience 33, 14526-14533.

Power, J.D., Mitra, A., Laumann, T.O., Snyder, A.Z., Schlaggar, B.L., Petersen, S.E., 2014. Methods to detect, characterize, and remove motion artifact in resting state fMRI. Neuroimage 84, 320-341.

Regenbogen, C., Vos, M., Debener, S., Turetsky, B.I., Mößnang, C., Finkelmeyer, A., Habel, U., Neuner, I., Kellermann, T., 2012. Auditory Processing under Cross-Modal Visual Load Investigated with Simultaneous EEG-fMRI. PLoS One 7.

Rice, J.K., Rorden, C., Little, J.S., Parra, L.C., 2013. Subject position affects EEG magnitudes. Neuroimage 64, 476-484.

Ritter, P., Moosmann, M., Villringer, A., 2009. Rolandic alpha and beta EEG rhythms' strengths are inversely related to fMRI-BOLD signal in primary somatosensory and motor cortex. Hum Brain Mapp 30, 1168-1187.

Sadaghiani, S., Scheeringa, R., Lehongre, K., Morillon, B., Giraud, A.L., Kleinschmidt, A., 2010. Intrinsic connectivity networks, alpha oscillations, and tonic alertness: a simultaneous electroencephalography/functional magnetic resonance imaging study. J Neurosci 30, 10243-10250.

Sammer, G., Blecker, C., Gebhardt, H., Bischoff, M., Stark, R., Morgen, K., Vaitl, D., 2007. Relationship between regional hemodynamic activity and simultaneously recorded EEG-theta associated with mental arithmetic-induced workload. Hum Brain Mapp 28, 793-803.

Satterthwaite, T.D., Wolf, D.H., Ruparel, K., Erus, G., Elliott, M.A., Eickhoff, S.B., Gennatas, E.D., Jackson, C., Prabhakaran, K., Smith, A., Hakonarson, H., Verma, R., Davatzikos, C., Gur, R.E., Gur, R.C., 2013. Heterogeneous impact of motion on fundamental patterns of developmental changes in functional connectivity during youth. Neuroimage 83, 45-57.

Scheeringa, R., Fries, P., Petersson, K.M., Oostenveld, R., Grothe, I., Norris, D.G., Hagoort, P., Bastiaansen, M.C., 2011. Neuronal dynamics underlying high- and low-frequency EEG oscillations contribute independently to the human BOLD signal. Neuron 69, 572-583.

Scheeringa, R., Petersson, K.M., Oostenveld, R., Norris, D.G., Hagoort, P., Bastiaansen, M.C., 2009. Trial-by-trial coupling between EEG and BOLD identifies networks related to alpha and theta EEG power increases during working memory maintenance. Neuroimage 44, 1224-1238.

Shmueli, K., van Gelderen, P., de Zwart, J.A., Horovitz, S.G., Fukunaga, M., Jansma, J.M., Duyn, J.H., 2007. Low-frequency fluctuations in the cardiac rate as a source of variance in the resting-state fMRI BOLD signal. Neuroimage 38, 306-320.

Siegel, J.S., Power, J.D., Dubis, J.W., Vogel, A.C., Church, J.A., Schlaggar, B.L., Petersen, S.E., 2014. Statistical improvements in functional magnetic resonance imaging analyses produced by censoring high-motion data points. Hum Brain Mapp 35, 1981-1996.

Staudigl, T., Hanslmayr, S., 2013. Theta oscillations at encoding mediate the context-dependent nature of human episodic memory. Curr Biol 23, 1101-1106.

Thibault, R.T., Lifshitz, M., Jones, J.M., Raz, A., 2014. Posture alters human resting-state. Cortex 58, 199-205.

van Buuren, M., Gladwin, T.E., Zandbelt, B.B., van den Heuvel, M., Ramsey, N.F., Kahn, R.S., Vink, M., 2009. Cardiorespiratory effects on default-mode network activity as measured with fMRI. Hum Brain Mapp 30, 3031-3042.

van der Meer, J.N., Pampel, A., Someren, E., Ramautar, J.R., van der Werf, Y.D., Gomez-Herrero, G., Lepsien, J., Hellrung, L., Hinrichs, H., Möller, H.E., Walter, M., 2015. Carbon-wire loop based artifact correction outperforms post-processing EEG/fMRI corrections—A validation of a real-time simultaneous EEG/fMRI correction method. Neuroimage.

Vlemincx, E., Taelman, J., De Peuter, S., Van Diest, I., Van den Bergh, O., 2011. Sigh rate and respiratory variability during mental load and sustained attention. Psychophysiology 48, 117-120.

White, T.P., Jansen, M., Doege, K., Mullinger, K.J., Park, S.B., Liddle, E.B., Gowland, P.A., Francis, S.T., Bowtell, R., Liddle, P.F., 2013. Theta power during encoding predicts subsequent-memory performance and default mode network deactivation. Hum Brain Mapp 34, 2929-2943.

Yan, C.G., Cheung, B., Kelly, C., Colcombe, S., Craddock, R.C., Di Martino, A., Li, Q., Zuo, X.N., Castellanos, F.X., Milham, M.P., 2013. A comprehensive assessment of regional variation in the impact of head micromovements on functional connectomics. Neuroimage 76, 183-201.

Yan, W.X., Mullinger, K.J., Brookes, M.J., Bowtell, R., 2009. Understanding gradient artefacts in simultaneous EEG/fMRI. Understanding gradient artefacts in simultaneous EEG/fMRI.

Yan, W.X., Mullinger, K.J., Geirsdottir, G.B., Bowtell, R., 2010. Physical modeling of pulse artefact sources in simultaneous EEG/fMRI. Human Brain Mapping 31, 604-620.

Yuan, H., Zotev, V., Phillips, R., Bodurka, J., 2013. Correlated slow fluctuations in respiration, EEG, and BOLD fMRI. Neuroimage 79, 81-93.

Zotev, V., Yuan, H., Phillips, R., Bodurka, J., 2012. EEG-assisted retrospective motion correction for fMRI: E-REMCOR. Neuroimage 63, 698-712.

Zumer, J.M., Scheeringa, R., Schoffelen, J.M., Norris, D.G., Jensen, O., 2014. Occipital alpha activity during stimulus processing gates the information flow to object-selective cortex. PLoS Biol 12, e1001965.